

Deviations from the Porter-Thomas distribution due to non-statistical γ decay below the ^{150}Nd neutron separation threshold

O. Papst ^{1,*} J. Isaak ^{1,†} V. Werner ¹ D. Savran ² N. Pietralla ¹ G. Battaglia ³ T. Beck ^{1,‡}
M. Beuschlein ¹ S. W. Finch ^{4,5} U. Friman-Gayer ^{1,§} K. E. Ide ¹ R. V. F. Janssens ^{5,6} M. D. Jones^{5,6}
J. Kleemann ¹ B. Löher ² M. Scheck ^{7,8} M. Spieker ^{9,¶} W. Tornow ^{4,5} R. Zidarova ¹ and A. Zilges ¹⁰

¹Technische Universität Darmstadt, Department of Physics, Institute for Nuclear Physics, 64289 Darmstadt, Germany

²GSI Helmholtzzentrum für Schwerionenforschung GmbH, 64291 Darmstadt, Germany

³University of Strathclyde, Glasgow G4 0NG, United Kingdom

⁴Department of Physics, Duke University, Durham, NC 27708-0308, USA

⁵Triangle Universities Nuclear Laboratory, Durham, NC 27708-0308, USA

⁶Department of Physics and Astronomy, University of North Carolina at Chapel Hill, Chapel Hill, NC 27599, USA

⁷School of Computing, Engineering, and Physical Sciences, University of the West of Scotland, Paisley PA1 2BE, United Kingdom

⁸The Scottish Universities Physics Alliance, Glasgow G12 8QQ, United Kingdom

⁹National Superconducting Cyclotron Laboratory, Michigan State University, East Lansing, MI 48824, USA

¹⁰Institut für Kernphysik, Universität zu Köln, 50937 Köln, Germany

(Dated: January 1, 2025)

We introduce a new method for the study of fluctuations of partial transition widths based on nuclear resonance fluorescence experiments with quasimonochromatic linearly-polarized photon beams below particle separation thresholds. It is based on the average branching of decays of $J = 1$ states of an even-even nucleus to the 2_1^+ state in comparison to the ground state. Between 5 and 7 MeV, an almost constant average branching ratio of 0.490(16) is observed for the nuclide ^{150}Nd . Assuming χ^2 -distributed partial transition widths, this average branching ratio is related to a degree of freedom of $\nu = 1.93(12)$, rejecting the validity of the Porter-Thomas distribution, requiring $\nu = 1$. The observed deviation can be explained by non-statistical effects in the γ -decay behavior with contributions in the range of 9.4(10) % up to 94(10) %.

Introduction.—Random Matrix Theory (RMT) provides a comprehensive framework for the description of complex, chaotic quantum systems, such as those found in nuclear physics [1], and is widely applicable across various domains of physics [2]. The RMT is an integral part of the statistical treatment of nuclear reactions and, thus, its validity is of considerable importance for the calculation of reaction cross sections. Originally developed by Wigner [3] and Dyson [4–6], RMT assumes a Hamiltonian matrix with randomly distributed matrix elements and allows for the extraction of statistical properties such as the distribution of nuclear level spacings and partial transition widths. Of particular interest are Gaussian-distributed matrix elements, resulting in χ^2 -distributed partial transition widths Γ_i (see Supplementary Material [7]). The symmetries conserved by the interaction determine the degree of freedom ν of the χ^2 distribution. For integer-valued angular momentum and good time-reversal symmetry, an orthogonal Hamiltonian with a Gaussian orthogonal ensemble (GOE) is obtained, resulting in a χ^2 distribution with one degree of freedom ($\nu = 1$), which is commonly referred to as the Porter-Thomas (PT) distribution [8].

The applicability of the PT distribution of partial transition widths has been extensively studied in thermal neutron capture experiments [9–21]. An analysis of the nuclear data ensemble (NDE) of neutron resonances [9] to validate the PT distribution finds good agreement between GOE-predictions and experimental data. However, studies on ^{26}Al and ^{30}P below 8 MeV [10, 11] revealed significant deviations from PT predictions. Koehler *et al.* [14] found a degree of freedom of $\nu \approx 0.5$ from neutron-resonance spacings of Pt isotopes, sig-

nificantly smaller than $\nu = 1$. A subsequent reanalysis of the NDE reported $\nu = 0.80(5)$ [16]. After correcting for p -wave contamination, $\nu = 1.22(9)$ is obtained, still deviating from the PT prediction, but in the opposite direction. In another experiment, for ^{147}Sm , ν changed abruptly from $\nu = 1.04^{+0.33}_{-0.31}$ to $\nu = 2.7(6)$ for neutron-resonance widths slightly above the neutron-separation threshold [12, 13, 18]. In Ref. [19], coupling to other decay channels such as non-statistical γ decays has been shown to result in a significant modification of width distributions, with the effective Hamiltonian comprising a GOE term and a coupling term with broken orthogonal symmetry.

To date, no experimental data exists for width fluctuations below neutron separation thresholds. This region is particularly interesting because it contains the onset of the quasi-continuum region, where the nuclear spectra transition from a few individual states at low excitation energies to an ensemble of states at high excitation energies which can be described by the ansatz of the Hauser-Feshbach statistical model [22]. Photon-scattering experiments below particle thresholds are frequently used to extract information on photon strength functions (PSF) [23] and other γ -decay properties, which are an essential input for calculations in the Hauser-Feshbach statistical model, e.g., in nuclear reaction model codes such as TALYS-2.0 [24].

In this Letter, we present a new method for the study of fluctuations of partial transition widths, which relates the average branching ratio of internal γ decays to the degree of freedom of the χ^2 distribution. Using quasimonochromatic, linearly-polarized photon beams, photon scattering experiments be-

low particle separation thresholds are performed. This energy region is primarily associated with the concentration of $E1$ strength called the pygmy dipole resonance (PDR) [25–27]. At high excitation energies, sufficiently high nuclear level densities (NLD) prevent the spectral resolution of the decay from most excited levels, which can no longer be resolved individually and instead appear as a single broad “hump” resembling the spectral distribution of the incoming photon beam.

Experiment and results.—Nuclear resonance fluorescence (NRF) experiments [28, 29] have been performed at the Triangle Universities Nuclear Laboratory (TUNL) with the High Intensity γ -ray Source (HI γ S) [30]. The facility provides quasi-monochromatic photon beams from laser-Compton backscattering (LCB) in the MeV range. The machine was operated in a new high-resolution mode that reduces the spectral bandwidth of the photon beam to about 1.8% by optimizing the electron beam parameters and using narrower collimators at the expense of photon-flux intensity. The linearly-polarized, quasimonochromatic MeV-ranged photon beams were scattered off a target composed of 11.583(1) g of Nd_2O_3 enriched to 93.60(2)% of ^{150}Nd . The target was mounted in the γ^3 setup for γ -ray spectroscopy [31] equipped with four high-purity germanium (HPGe) detectors placed at azimuthal angles ϑ and polar angles φ with respect to the horizontal polarization plane of $(\vartheta, \varphi) \in \{(90^\circ, 90^\circ), (90^\circ, 180^\circ), (135^\circ, 45^\circ), (135^\circ, 315^\circ)\}$ and four lanthanum bromide (LaBr_3) detectors placed at $(\vartheta, \varphi) \in \{(90^\circ, 0^\circ), (90^\circ, 270^\circ), (135^\circ, 135^\circ), (135^\circ, 225^\circ)\}$. A further “zero-degree” HPGe detector was briefly inserted into the (attenuated) photon beam to measure the spectral distribution for each photon beam energy setting.

For ^{150}Nd , which is close to the shape phase transition from spherical to prolate-deformed nuclei [32], the energy of the 2_1^+ state of 130 keV in combination with the recently developed high-resolution mode allowed for the separation of all transitions from excited states to the ground state band. The collimator radius was reduced from 9.525 mm to 5 mm in accordance with the photon beam energy increase from 3 MeV to 7 MeV, ensuring the separability of decays from excited states to the 0_1^+ ground state and the 2_1^+ state in integral spectroscopy [33, 34], i.e., without resolving individual transitions at all beam energies.

The high-resolution mode of the LCB beam significantly reduces the overlap between the two energy regions containing transitions from excited states to the 0_1^+ state and to the 2_1^+ state, respectively (see Fig. 1). A fit-based method was used to separate both contributions and decompose the spectrum into its individual components. This was combined with the correction of the detector response into a single optimization procedure per energy setting, taking into account data from all detectors. It was assumed that the fragmentation of states in the studied energy range is high, such that the excitation strength is distributed approximately uniformly across the excited energy range defined by the beam energy profile. As a consequence, individual transitions are no longer resolved. The shape of the ground-state decays (“hump”) is expected to closely resemble the shape of the spectral distribution of the photon beam. The

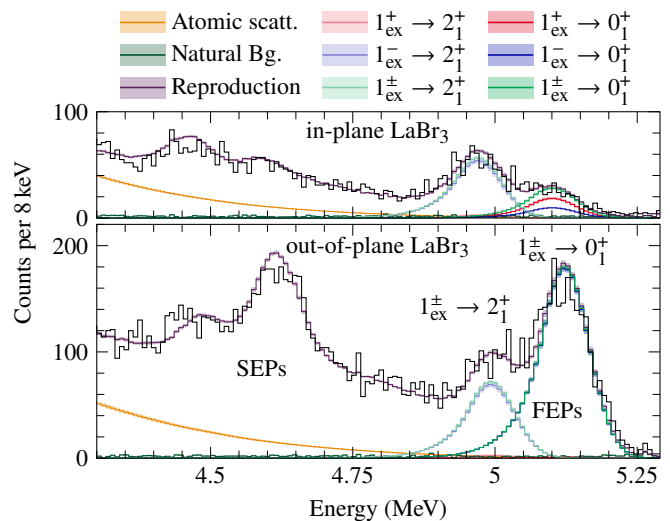


FIG. 1. Detector response correction and decomposition of ^{150}Nd spectra for two LaBr_3 detectors. The fit-based reproduction is compared to the original spectrum. In addition, the fitted individual contributions to each spectrum are shown. The energy ranges of full-energy peaks (FEPs) and single-escape peaks (SEPs) are indicated.

photon beam distribution was directly measured for each photon beam energy setting using the zero-degree detector measurement, and subsequently corrected for using the respective detector response. A second hump, shifted to a lower energy by the excitation energy of the 2_1^+ state of $E(2_1^+) \approx 130$ keV, corresponds to decays of excited states to the 2_1^+ state. Each hump consists of contributions from excited 1^+ and 1^- states (assuming contributions by $J > 1$ states to be negligible), each with its own distinct angular distribution [35, 36] with respect to HI γ S’s linearly-polarized photon beam [37]. The (angular-distribution specific) detector response matrix was simulated for each detector using GEANT4 [38–40]. To reproduce the observed spectrum, the detector response is applied separately to the four decay branches. Natural background radiation and atomic scattering of the photon beam from the target result in further contributions, although these are negligible in the vicinity of the full-energy peak. NRF reactions on ^{12}C and ^{16}O target contaminations are also corrected for using their respective detector responses and angular distributions. The fit parameters are the number of counts of the four humps ($1^+ \rightarrow 0_1^+$, $1^- \rightarrow 0_1^+$, $1^+ \rightarrow 2_1^+$, $1^- \rightarrow 2_1^+$). The fit simultaneously minimizes the deviation between the observed spectra and the reproduction for all detectors, taking into account the observed background.

The measured experimental average cross sections σ^{exp} are the sum of non-resonant elastic scattering processes and NRF processes [41], $\sigma^{\text{exp}} \approx \sigma^{\text{coh}} + \sigma^{\text{NRF}}$. For low NLDs without overlapping levels, this equality is exact [42]. Only at higher NLDs in the continuum-region of, e.g., the isovector giant dipole resonance (IVGDR) [43, 44], an additional term arises from the interference between coherent elastic scattering and NRF scattering amplitudes [45, 46]. In the absence of overlap-

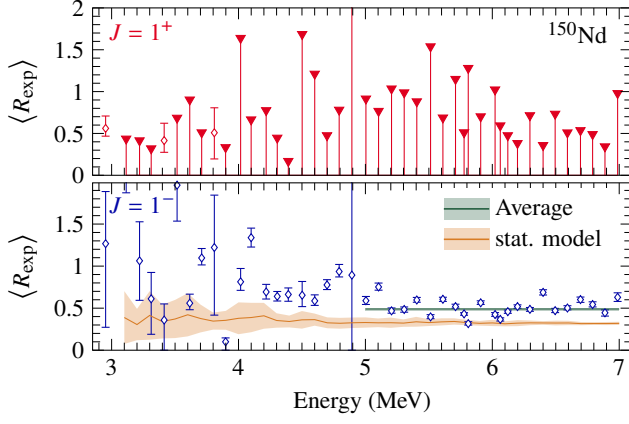


FIG. 2. Average branching ratios $\langle R_{\text{exp}} \rangle$ for ^{150}Nd for 1^- and 1^+ states. The latter can only be given as 2σ upper limits for most energies based on the angular distribution analysis. For lower photon beam energies up to around 4 MeV to 5 MeV, the fit-based method to determine the branching ratios is less reliable because of low NLDs and results in further systematic uncertainties that are not included in the pictured uncertainty intervals. A statistical model simulation based on the DICEBOX code [49] is also shown. See text for additional details.

ping NRF resonances, the contributions from constructive and destructive interference cancel each other out in integral spectroscopy and the interference term vanishes. Multiple coherent elastic scattering processes can occur: Delbrück, Rayleigh, and Thomson scattering. Delbrück and Rayleigh scattering can be neglected for the photon beam energies and detector positions utilized for this experiment [47] because they are expected to become significant only at very forward scattering angles. Only nuclear Thomson scattering contributes significantly to the experimentally observed cross sections [48], with an angular distribution indistinguishable from $E1$ ground-state transitions for an even-even nucleus. Thus, averaged cross sections for $E1$ ground-state transitions, as determined by the aforementioned fit procedure, were corrected by the energy-independent Thomson cross section of $\sigma^{\text{Thomson}} = 0.115$ mb calculated for ^{150}Nd . A table with the experimental results for the integral spectroscopy analysis can be found in the supplemental material [7, 50].

The measured average branching ratio defined in this work

$$\langle R_{\text{exp}} \rangle = \frac{\sum_i I_{2,i}}{\sum_i I_{0,i}} \cdot \frac{E_{\gamma_0}^3}{E_{\gamma_2}^3} = \frac{\sum_i \Gamma_{0,i} \frac{\Gamma_{2,i}}{\Gamma_i}}{\sum_i \Gamma_{0,i} \frac{\Gamma_{0,i}}{\Gamma_i}} \cdot \frac{E_{\gamma_0}^3}{E_{\gamma_2}^3} \quad (1)$$

depends on the energy-integrated NRF cross sections $I_{2,i}$ and $I_{0,i}$ for photoexcitation of a state i from the ground state and subsequent decay to the 2_1^+ state and to the ground state, respectively. It is also dependent on $\Gamma_{0,i}$, $\Gamma_{2,i}$, and Γ_i , which are the partial transition widths to the ground state, to the 2_1^+ state, and the total transition width of all levels i populated in a given excitation energy range, respectively. The average γ -ray transition energies to the ground state and to the 2_1^+ state are given by E_{γ_0} and E_{γ_2} , respectively, and are set equal for

all states in the narrow excitation energy region defined by the photon beam. Experimentally, it is determined as

$$\langle R_{\text{exp}} \rangle = \frac{A_{1^- \rightarrow 2^+}}{A_{1^- \rightarrow 0^+}} \cdot \frac{\varepsilon(E_{\gamma_0}) W_{0^+ \rightarrow 1^- \rightarrow 0^+}}{\varepsilon(E_{\gamma_2}) W_{0^+ \rightarrow 1^- \rightarrow 2^+}} \cdot \frac{E_{\gamma_0}^3}{E_{\gamma_2}^3}, \quad (2)$$

with the total number of observed counts A_x for the hump belonging to transition x , angular distribution coefficients W_x , and detector efficiencies $\varepsilon(E_\gamma)$ for energy E_γ . The experimental $\langle R_{\text{exp}} \rangle$ values are depicted in the lower (upper) panel for 1^- (1^+) in Fig. 2. The angular distributions for $0^+ \rightarrow 1^\pm \rightarrow 2^+$ cascades are considerable less pronounced than those observed for ground-state transitions. Consequently, the sensitivity to the parity of excited states is reduced. Most of the decays to the 2^+ states are attributed to 1^- states. Upper limits are given for decays of 1^+ states at most energies, given that 1^- states dominate the ground-state transitions. At lower excitation energies, up to approximately 4 to 5 MeV, the average branching ratios for 1^- states vary strongly, and their uncertainties are large. This phenomenon can be explained by the low NLD, which violates the assumption employed in the fit procedure that the strength is distributed uniformly across the excitation energy region and, thus, the decay properties of individual states dominate the branchings. The situation is distinct for excitation energies exceeding 5 MeV where increasing NLD lead to reliable results for the average branching ratios. In this region, the $\langle R_{\text{exp}} \rangle$ values do not vary strongly and converge upon a common value of about 0.5.

For the following analysis, a constant average value for $\langle R_{\text{exp}} \rangle$ for energies above 5 MeV was determined using a Bayesian approach. In order to account for the scatter of the data points, their variance was assumed to be unknown and inverse-gamma distributed, resulting in the Student's t -distribution. An average value of $\langle \langle R_{\text{exp}} \rangle \rangle = 0.490(16)$ was determined.

Discussion.—In the following, the observed average branching ratios are discussed in light of the statistical Hauser-Feshbach model [22]. The partial transition widths $\Gamma_{j,i}$ in Eq. (1) are assumed to be χ^2 distributed (normalized to unit expectation) and can be expressed as $\Gamma_{j,i} = \langle \Gamma_j \rangle \cdot f_i$ for a $0_1^+ \rightarrow 1_i^\pm \rightarrow J_j^+$ cascade, where f_i is a χ^2 -distributed random variable normalized to its degree of freedom ν . The total transition widths are sums of χ^2 -distributed quantities, which can be approximated using a Gaussian distribution represented by the random variable g_i , if more than three partial widths contribute to each Γ_i . Thus, one can transform the ratio of sums of partial and total transition widths in Eq. (1) into

$$\frac{\sum_i \Gamma_{0,i} \frac{\Gamma_{2,i}}{\Gamma_i}}{\sum_i \Gamma_{0,i} \frac{\Gamma_{0,i}}{\Gamma_i}} = \frac{\langle \Gamma_2 \rangle \sum_i f_i \cdot f'_i / g_i}{\langle \Gamma_0 \rangle \sum_i f_i \cdot f_i / g_i} = \frac{\langle \Gamma_2 \rangle}{\langle \Gamma_0 \rangle} s \quad (3)$$

$$\Rightarrow s \equiv \frac{\sum_i f_i \cdot f'_i / g_i}{\sum_i f_i \cdot f_i / g_i} \quad (4)$$

The quantity is separated into a factor that depends on the ratio of average partial transition widths to the ground state (2_1^+ state), given by $\langle \Gamma_0 \rangle$ ($\langle \Gamma_2 \rangle$) and the internal fluctuation

ratio s . The latter is sensitive to the statistical distribution of partial transition widths of excited states. For χ^2 distributions, the internal fluctuation ratio s can be directly related [7] to the degree of freedom ν via

$$s = \frac{\nu}{\nu + 2} \quad \Leftrightarrow \quad \nu = \frac{2s}{1 - s}. \quad (5)$$

A detailed analysis of the convergence of s as a function of the number of excited states and decay branches can be found in the supplementary material [7]. Assuming all partial widths being independently PT distributed, i.e., $\nu = 1$, a value of $s = 1/3$ is obtained; see Refs. [51, 52] for similar conclusions. If the ground-state decays are substituted by decays to any other state in Eq. (3), a value of $s = 1$ is obtained.

As a result, under the assumption that all observed transitions are accurately described by the statistical model, i.e. given all partial transition widths follow the same χ^2 distribution, $\langle R_{\text{exp}} \rangle$ can be related to s via

$$\langle R_{\text{exp}} \rangle = s \frac{\langle \Gamma_2 \rangle E_{\gamma_0}^3}{\langle \Gamma_0 \rangle E_{\gamma_2}^3} = s \frac{f_{E1}(E_{\gamma_2})}{f_{E1}(E_{\gamma_0})} \quad (6)$$

with $f_{E1}(E_{\gamma_i}) \propto \langle \Gamma_i \rangle / E_{\gamma_i}^3$ [23, 52] being the PSF for $E1$ transitions with γ -ray energies E_{γ_i} . Because of the low energy of the 2_1^+ state of ^{150}Nd , assuming the validity of the Brink-Axel (BA) hypothesis [51, 53], f_{E1} changes typically less than 3% within the 130 keV difference between decays to the 0_1^+ state and to the 2_1^+ state in the region of interest from 5 to 7 MeV. Consequently, in a case of a typical deformed rare-earth nucleus like ^{150}Nd with a low $E(2_1^+)$, Eq. (6) can be approximated by $\langle R_{\text{exp}} \rangle \approx s$.

To validate the formalism derived above, a statistical model simulation was performed using a version of the Monte-Carlo method-based DICEBOX code [49] adapted for the simulation of γ -ray cascades in NRF reactions. Starting from the 12 lowest-lying experimentally known levels of ^{150}Nd [54], an artificial nucleus is generated (a so-called realization) with a random level scheme with partial decay widths for each level following PT fluctuations. The average decay behavior follows the statistical properties defined by the input NLD and PSF. In order to calculate the NLD, the back-shifted Fermi gas model is employed, with parameters $E1 = -0.516$ MeV and $a = 16.275$ MeV $^{-1}$ taken from Ref. [55]. The input PSFs are composed of the IVGDR (standard Lorentzians, parametrized according to Ref. [56]) for $E1$ contributions, scissors and spin-flip resonance parametrized by the SMLO model [57] to account for $M1$ transitions and negligible $E2$ contributions from single-particle contributions. For each photon beam energy setting of the experiment, the population of excited states via the NRF reaction is simulated in accordance to the actual spectral distribution of the photon beam. The subsequent decay of these states via γ -ray cascades is simulated and analyzed in the same way as the experimental data. Due to the low energy of the 2_1^+ state, the results of the statistical model simulation for the average branching ratio are not sensitive to the PSF and

NLD model parameters, and the same results can be obtained with any sensible combination of values.

The entire process is repeated for a total of 30 different realizations. For each photon beam energy setting, $\langle R_{\text{sim}} \rangle$ is extracted from the simulations in a manner analogous to the experimental results of this work. In the lower panel of Fig. 2, a comparison of the simulated $\langle R_{\text{sim}} \rangle$ (red solid line and uncertainty band) and the experimental results is presented. For both experiment and simulation, the average $E1$ branching ratio stays approximately constant between 5 and 7 MeV. The simulation yielded $\langle R_{\text{sim}} \rangle \approx 0.31$, which is in excellent agreement with the internal fluctuation ratio of $s = 1/3$ required for PT-distributed partial transition widths. Thus, it follows that the derivation of s and the approximations that lead to $\langle R_{\text{exp}} \rangle \approx s$ are well justified.

For the experimental result of $\langle \langle R_{\text{exp}} \rangle \rangle = 0.490(16)$ above 5 MeV, a value of $\nu = 1.93(12)$ is obtained using Eq. (5). This value is considerably larger than $\nu = 1$ and, thus, does not agree with the PT distribution within seven standard deviations. Photon strength functions are usually parametrized with (modified) Lorentzian functions [23] and, thus, typically increase monotonically with γ -ray energy, i.e. $f_{E1}(E_{\gamma_2})/f_{E1}(E_{\gamma_0}) < 1$, leading to even larger values for s and, consequently, ν . It can therefore be concluded that the assumptions of the statistical model are inconsistent with the experimental observations.

Besides a modified statistical distribution of partial transition widths, namely a modified degree of freedom ν of the χ^2 distribution, other explanations may account for the observed deviations: The assumption of large NLDs (> 100 levels per MeV) could be violated, or strong non-statistical decays could skew the resulting distribution of partial transition widths in a way that cannot be described by the χ^2 distribution.

A potential non-statistical contribution to the observed decay behavior may arise from the decay pattern of nuclear states in a well-deformed nucleus, according to the Alaga rule [58]. The decay intensity for transitions to the ground-state rotational band depends on the excited states' quantum number K , where K is the projection of the total angular momentum onto the symmetry axis of the nucleus. For $K = 0$ states, the expected branching ratio is $\Gamma_2/\Gamma_0 \cdot (E_{\gamma_0}/E_{\gamma_2})^3 = 2.0$, while for $K = 1$ states it is $\Gamma_2/\Gamma_0 \cdot (E_{\gamma_0}/E_{\gamma_2})^3 = 0.5$. The experimental branching ratios below 4 MeV for ^{150}Nd were found to be in good agreement with the Alaga rules [59]. Previous studies on deformed nuclei exhibit a preference for $K = 0$ for low-energy 1^- states below 4 MeV [60]. To estimate the strength from non-statistically decaying states, $\langle R_{\text{exp}} \rangle$ can be separated

$$\langle R_{\text{exp}} \rangle = s \frac{f_{E1}(E_{\gamma_2})}{f_{E1}(E_{\gamma_0})} C_{\text{stat}} + 2C_{K=0} + 0.5C_{K=1} \quad (7)$$

into fractions of the ground-state decay cross section that arise from excited 1^- states that decay statistically (C_{stat}), as expected from pure $K = 0$ states ($C_{K=0}$), and $K = 1$ states ($C_{K=1}$) with the identity $C_{\text{stat}} + C_{K=0} + C_{K=1} = 1$. A detailed derivation is provided in the Supplemental Material [7].

Assuming that only $K = 0$ states contribute to the non-statistical part, i.e. $C_{K=1} = 0$, using $\langle \langle R_{\text{exp}} \rangle \rangle = 0.490(16)$

and $s = 1/3$, one finds that even a small contribution of $C_{K=0} = 9.4(10)\%$ of the total ground-state decay cross section from $K = 0$ states is sufficient to explain the experimental observations. It is important to note that this value marks a lower limit of the non-statistical contribution. An upper limit of $C_{K=1} = 94(10)\%$ is obtained, if solely $K = 1$ states would contribute, implying $C_{K=0} = 0$.

These new findings strongly support previous evidence that the γ -ray decay properties of photoexcited states in the quasicontinuum regime do not follow the expectations from the extreme statistical model [33, 61–64]. In addition, fluctuation properties of partial widths, especially for the ground-state decay channel, need to be treated correctly in NRF reactions. If average branching ratios $\langle R_{\text{exp}} \rangle$ are related to the ratio of PSFs, the internal fluctuation ratio s must be taken into account. This is especially important if values for PSFs are extracted via the ratio or shape method [65, 66]. As noted above, this only affects the ground-state decay channel, as $s = 1$ for the ratio of transitions not involving the decay to the ground state.

The photoabsorption cross section of ^{150}Nd reveals a pronounced double-humped structure in the region of its isovector giant dipole resonance (IVGDR) [56]. In more recent experiments, the observed splitting is less pronounced [67]. This splitting of the IVGDR is widely regarded as a signature of nuclear deformation and is attributed to axial deformation, which enables proton-neutron vibrations to occur parallel ($K = 0$) and perpendicular ($K = 1$) relative to the nuclear symmetry axis with different associated frequencies [68, 69]. Recent observations of the γ -decay from the IVGDR in the well-deformed nucleus ^{154}Sm revealed a distinct variation of $\langle R_{\text{exp}} \rangle$ across the two humps identified as the $K = 0$ and $K = 1$ IVGDR components [46]. In hydrodynamical models, the PDR is usually interpreted as a collective oscillation of a neutron skin relative to an inert isospin-saturated core. Accordingly, a splitting of the PDR strength in deformed nuclei, analogous to the behavior observed for the IVGDR, might be anticipated [27]. It is noteworthy, that from a theoretical point of view the effect of the deformation on the dipole response in the region of the PDR is not conclusive at all [27]. The present study finds a constant value of $\langle R_{\text{exp}} \rangle = 0.490(16)$ in the energy region from 5 to 7 MeV for ^{150}Nd , with no evidence of a gradual transition between regions corresponding to different K -quantum numbers, as observed in the IVGDR of ^{154}Sm [46]. Consequently, the data presented here for the energy region below 7 MeV provide no indication of a pronounced splitting of the $E1$ strength into K components in the PDR region of ^{150}Nd .

Summary.— For the first time, the statistical distribution of partial transition widths below particle separation thresholds could be probed based on NRF experiments utilizing the new high-resolution HI γ S operating mode. An internal fluctuation ratio of $s = 0.490(16)$ was observed, which differs significantly from the $s = 1/3$ prediction for PT-distributed partial transition widths and confirmed by statistical model simulations. Assuming χ^2 -distributed partial transition widths, the observed internal fluctuation ratio is associated with a degree of freedom of $\nu = 1.93(12)$ in clear disagreement with the

PT distribution. We illustrated that contributions as small as 9.4(10)%, and up to 94(10)%, from non-statistical decays, in addition to a PT-distributed fraction, can significantly alter the experimental observations.

We would like to thank A. Leviatan for useful comments and discussions. We thank S. Bassauer, M. Berger, P. C. Ries, E. Hoemann, N. Kelly, R. Kern, Krishichayan, D. R. Little, M. Müscher, J. Sinclair, and J. Wiederhold for help with the data taking. We thank the HI γ S accelerator crew for providing excellent photon beams for our experiment. The ^{150}Nd target was supplied by the Isotope Program within the Office of Nuclear Physics in the U.S. Department of Energy’s Office of Science. This work has been funded by the Deutsche Forschungsgemeinschaft (DFG, German Research Foundation) – Project-ID 279384907 – SFB 1245, Project-ID 460150577 – ZI 510/10-1, and Project-ID 499256822 – GRK 2891 “Nuclear Photonics”, by the State of Hesse under the grant “Nuclear Photonics” within the LOEWE program (LOEWE/2/11/519/03/04.001(0008)/62), by the BMBF under grant number 05P21RDEN9, and by the U.S. Department of Energy, Office of Science, Office of Nuclear Physics, under grants DE-SC0023010, DE-FG02-97ER41041 (UNC), and DE-FG02-97ER41033 (TUNL). M. Scheck acknowledges financial support by the UK-STFC (Grant No. ST/P005101/1).

* opapst@ikp.tu-darmstadt.de

† jisaak@ikp.tu-darmstadt.de

‡ Present address: Laboratoire de Physique Corpusculaire, ISMRA and Université de Caen, IN2P3-CNRS, 14050 Caen Cedex, France

§ Present address: Vysus Group Sweden AB, 214 21 Malmö, Sweden

¶ Present address: Department of Physics, Florida State University, Tallahassee, FL 32306, USA

- [1] H. A. Weidenmüller and G. E. Mitchell, *Rev. Mod. Phys.* **81**, 539 (2009).
- [2] T. Guhr, A. Müller-Groeling, and H. A. Weidenmüller, *Phys. Rep.* **299**, 189 (1998).
- [3] E. P. Wigner, *Ann. of Math.* **62**, 548 (1955).
- [4] F. J. Dyson, *J. Math. Phys.* **3**, 140 (1962).
- [5] F. J. Dyson, *J. Math. Phys.* **3**, 157 (1962).
- [6] F. J. Dyson, *J. Math. Phys.* **3**, 166 (1962).
- [7] See Supplemental Material at <https://link.aps.org/supplemental/10.1103/PhysRevLett.XXX.0XXXXX> for tabulated experimental data presented in this article. It refers to Refs. [23, 52, 58, 70].
- [8] C. E. Porter and R. G. Thomas, *Phys. Rev.* **104**, 483 (1956).
- [9] R. U. Haq, A. Pandey, and O. Bohigas, *Phys. Rev. Lett.* **48**, 1086 (1982).
- [10] A. A. Adams, G. E. Mitchell, and J. F. Shriner, Jr, *Phys. Lett. B* **422**, 13 (1998).
- [11] J. F. Shriner, C. A. Grossmann, and G. E. Mitchell, *Phys. Rev. C* **62**, 054305 (2000).
- [12] P. E. Koehler, Y. M. Gledenov, T. Rauscher, and C. Fröhlich, *Phys. Rev. C* **69**, 015803 (2004).
- [13] P. E. Koehler, J. L. Ullmann, T. A. Bredeweg, J. M. O’Donnell, R. Reifarth, R. S. Rundberg, D. J. Vieira, and J. M. Wouters, *Phys. Rev. C* **76**, 025804 (2007).

- [14] P. E. Koehler, F. Bečvář, M. Krtička, J. A. Harvey, and K. H. Guber, *Phys. Rev. Lett.* **105**, 072502 (2010).
- [15] H. A. Weidenmüller, *Phys. Rev. Lett.* **105**, 232501 (2010).
- [16] P. E. Koehler, *Phys. Rev. C* **84**, 034312 (2011).
- [17] G. L. Celardo, N. Auerbach, F. M. Izrailev, and V. G. Zelevinsky, *Phys. Rev. Lett.* **106**, 042501 (2011).
- [18] P. E. Koehler, R. Reifarh, J. L. Ullmann, T. A. Bredeweg, J. M. O'Donnell, R. S. Rundberg, D. J. Vieira, and J. M. Wouters, *Phys. Rev. Lett.* **108**, 142502 (2012).
- [19] A. Volya, H. A. Weidenmüller, and V. Zelevinsky, *Phys. Rev. Lett.* **115**, 052501 (2015).
- [20] E. Bogomolny, *Phys. Rev. Lett.* **118**, 022501 (2017).
- [21] K. Hagino and G. F. Bertsch, *Phys. Rev. E* **104**, L052104 (2021).
- [22] W. Hauser and H. Feshbach, *Phys. Rev.* **87**, 366 (1952).
- [23] S. Goriely, P. Dimitriou, M. Wiedeking, T. Belgya, R. Firestone, J. Upecky, M. Krtička, V. Plujko, R. Schwengner, S. Siem, H. Utsunomiya, S. Hilaire, S. Péru, Y. S. Cho, D. M. Filipescu, N. Iwamoto, T. Kawano, V. Varlamov, and R. Xu, Reference database for photon strength functions, *Eur. Phys. J. A* **55**, 172 (2019).
- [24] A. Koning, S. Hilaire, and S. Goriely, *Eur. Phys. J. A* **59**, 10.1140/epja/s10050-023-01034-3 (2023).
- [25] D. Savran, T. Aumann, and A. Zilges, *Prog. Part. Nucl. Phys.* **70**, 210 (2013).
- [26] A. Bracco, E. Lanza, and A. Tamii, *Prog. Part. Nucl. Phys.* **106**, 360 (2019).
- [27] E. Lanza, L. Pellegrini, A. Vitturi, and M. Andrés, *Prog. Part. Nucl. Phys.* **129**, 104006 (2023).
- [28] F. R. Metzger, *Prog. Nucl. Phys.* **7**, 54 (1959).
- [29] A. Zilges, D. Balabanski, J. Isaak, and N. Pietralla, *Prog. Part. Nucl. Phys.*, 103903 (2021).
- [30] H. R. Weller, M. W. Ahmed, H. Gao, W. Tornow, Y. K. Wu, M. Gai, and R. Miskimen, *Prog. Part. Nucl. Phys.* **62**, 257 (2009).
- [31] B. Löher, V. Derya, T. Aumann, J. Beller, N. Cooper, M. Duchene, J. Endres, E. Fiori, J. Isaak, J. Kelley, M. Knörzer, N. Pietralla, C. Romig, M. Scheck, H. Scheit, J. Silva, A. P. Tonchev, W. Tornow, H. Weller, V. Werner, and A. Zilges, *Nucl. Instr. Meth. Phys. Res. A* **723**, 136 (2013).
- [32] R. Krücken, B. Albanna, C. Bialik, R. F. Casten, J. R. Cooper, A. Dewald, N. V. Zamfir, C. J. Barton, C. W. Beausang, M. A. Caprio, A. A. Hecht, T. Klug, J. R. Novak, N. Pietralla, and P. von Brentano, *Phys. Rev. Lett.* **88**, 232501 (2002).
- [33] J. Isaak, D. Savran, B. Löher, T. Beck, M. Bhihe, U. Gayer, Krishichayan, N. Pietralla, M. Scheck, W. Tornow, V. Werner, A. Zilges, and M. Zweidinger, *Physics Letters B* **788**, 225 (2019).
- [34] J. Isaak, D. Savran, B. Löher, T. Beck, U. Friman-Gayer, Krishichayan, N. Pietralla, V. Y. Ponomarev, M. Scheck, W. Tornow, V. Werner, A. Zilges, and M. Zweidinger, *Phys. Rev. C* **103**, 044317 (2021).
- [35] K. S. Krane, R. M. Steffen, and R. M. Wheeler, *At. Data Nucl. Data Tables* **11**, 351 (1973).
- [36] R. M. Steffen and K. Alder, in *The Electromagnetic Interaction in Nuclear Spectroscopy*, edited by W. D. Hamilton (North-Holland, Amsterdam, NL, 1975) Chap. 12, pp. 505–582.
- [37] N. Pietralla, H. R. Weller, V. N. Litvinenko, M. W. Ahmed, and A. P. Tonchev, *Nucl. Instrum. Meth. A* **483**, 556 (2002).
- [38] S. Agostinelli *et al.* (GEANT4 collaboration), *Nucl. Instr. Meth. Phys. Res. A* **506**, 250 (2003).
- [39] J. Allison *et al.* (GEANT4 collaboration), *IEEE Trans. Nucl. Sci.* **53**, 270 (2006).
- [40] J. Allison *et al.* (GEANT4 collaboration), *Nucl. Instr. Meth. Phys. Res. A* **835**, 186 (2016).
- [41] R. Leicht, M. Hammen, K. Schelhaas, and B. Ziegler, *Nucl. Phys. A* **362**, 111 (1981).
- [42] P. Rullhusen, U. Zurmühl, W. Mückenheim, F. Smend, M. Schumacher, and H. Börner, *Nucl. Phys. A* **382**, 79 (1982).
- [43] P. F. Bortignon, A. Bracco, and R. A. Broglia, *Giant Resonances: Nuclear Structure at Finite Temperature*, 1st ed., Contemporary concepts in physics, Vol. 10 (Harwood Academic Publishers, Reading, UK, 1998).
- [44] M. N. Harakeh and A. van der Woude, *Giant resonances: Fundamental high-frequency modes of nuclear excitation*, 1st ed., Oxford studies in nuclear physics, Vol. 24 (Clarendon Press, Oxford, UK, 2001).
- [45] S. Kahane, R. Moreh, and O. Shahal, *Phys. Rev. C* **28**, 1519 (1983).
- [46] J. Kleemann, N. Pietralla, U. Friman-Gayer, J. Isaak, O. Papst, K. Prifti, V. Werner, A. D. Ayangeakaa, T. Beck, G. Colò, M. L. Cortés, S. W. Finch, M. Fulghieri, D. Gribble, K. E. Ide, X. K. H. James, R. V. F. Janssens, S. R. Johnson, P. Koseoglou, Krishichayan, D. Savran, and W. Tornow, accepted for publication in *Phys. Rev. Lett.* (2024), arXiv:2406.19695 [nucl-ex].
- [47] P. Kane, L. Kissel, R. Pratt, and S. Roy, *Phys. Rep.* **140**, 75 (1986).
- [48] C. M. Davisson, *Interaction of γ -radiation with matter*, edited by K. Siegbahn, Alpha- Beta- and Gamma-ray Spectroscopy, Vol. 1 (North-Holland Publishing Company, 1965) Chap. II.
- [49] F. Bečvář, *Nucl. Instr. Meth. Phys. Res. A* **417**, 434 (1998).
- [50] O. Papst, J. Isaak, V. Werner, D. Savran, N. Pietralla, *et al.*, TUDatalib, Technische Universität Darmstadt (2025), <https://tudatalib.ulb.tu-darmstadt.de/handle/tudatalib/XXXX> (change in proof).
- [51] P. Axel, *Phys. Rev.* **126**, 671 (1962).
- [52] G. A. Bartholomew, E. D. Earle, A. J. Ferguson, J. W. Knowles, and M. A. Lone, Gamma-ray strength functions, in *Advances in Nuclear Physics*, Vol. 7, edited by M. Baranger and E. Vogt (Springer Science and Business Media LLC, New York, NY, USA, 1973) Chap. 4, pp. 229–324.
- [53] D. M. Brink, Phd thesis, Oxford University (1955).
- [54] S. Basu and A. A. Sonzogni, *Nucl. Data Sheets* **114**, 435 (2013).
- [55] T. von Egidy and D. Bucurescu, *Phys. Rev. C* **80**, 054310 (2009).
- [56] P. Carlos, H. Beil, R. Bergere, A. Lepretre, and A. Veyssiére, *Nucl. Phys. A* **172**, 437 (1971).
- [57] S. Goriely and V. Plujko, *Phys. Rev. C* **99**, 014303 (2019).
- [58] G. Alaga, K. Alder, A. Bohr, and B. R. Mottelson, *Dan. Mat. Fys. Medd.* **29** (1955).
- [59] H. Pitz, R. Heil, U. Kneissl, S. Lindenstruth, U. Seemann, R. Stock, C. Wesselborg, A. Zilges, P. von Brentano, S. Hoblit, and A. Nathan, *Nucl. Phys. A* **509**, 587 (1990).
- [60] D. Savran, S. Müller, A. Zilges, M. Babilon, M. W. Ahmed, J. H. Kelley, A. Tonchev, W. Tornow, H. R. Weller, N. Pietralla, J. Li, I. V. Pinayev, and Y. K. Wu, *Phys. Rev. C* **71**, 034304 (2005).
- [61] C. T. Angell, S. L. Hammond, H. J. Karwowski, J. H. Kelley, M. Krtička, E. Kwan, A. Makinaga, and G. Rusev, *Phys. Rev. C* **86**, 051302 (2012).
- [62] J. Isaak, D. Savran, M. Krtička, M. Ahmed, J. Beller, E. Fiori, J. Glorius, J. Kelley, B. Löher, N. Pietralla, C. Romig, G. Rusev, M. Scheck, L. Schnorrenberger, J. Silva, K. Sonnabend, A. Tonchev, W. Tornow, H. Weller, and M. Zweidinger, *Physics Letters B* **727**, 361 (2013).
- [63] O. Papst, V. Werner, J. Isaak, N. Pietralla, T. Beck, C. Bernards, M. Bhihe, N. Cooper, B. P. Crider, U. Friman-Gayer, J. Kleemann, Krishichayan, B. Löher, F. Naqvi, E. E. Peters, F. M. Prados-Estévez, R. S. Ilieva, T. J. Ross, D. Savran, W. Tornow, and J. R. Vanhoy, *Phys. Rev. C* **102**, 034323 (2020).
- [64] K. Sieja, *Eur. Phys. J. A* **59**, 147 (2023).
- [65] M. Wiedeking, L. A. Bernstein, M. Krtička, D. L. Bleuel, J. M. Allmond, M. S. Basunia, J. T. Harke, P. Fallon, R. B. Firestone,

- B. L. Goldblum, R. Hatarik, P. T. Lake, I.-Y. Lee, S. R. Leshner, S. Paschalis, M. Petri, L. Phair, and N. D. Scielzo, *Phys. Rev. Lett.* **108**, 162503 (2012).
- [66] M. Wiedeking, M. Guttormsen, A. C. Larsen, F. Zeiser, A. Görge, S. N. Liddick, D. Muecher, S. Siem, and A. Spyrou, *Phys. Rev. C* **104**, 014311 (2021).
- [67] L. Donaldson, C. Bertulani, J. Carter, V. Nesterenko, P. von Neumann-Cosel, R. Neveling, V. Ponomarev, P.-G. Reinhard, I. Usman, P. Adsley, J. Brummer, E. Buthelezi, G. Cooper, R. Fearick, S. Förtsch, H. Fujita, Y. Fujita, M. Jingo, W. Kleinig, C. Kureba, J. Kvasil, M. Latif, K. Li, J. Mira, F. Nemulodi, P. Papka, L. Pellegrini, N. Pietralla, A. Richter, E. Sideras-Haddad, F. Smit, G. Steyn, J. Swartz, and A. Tamii, *Phys. Lett. B* **776**, 133 (2018).
- [68] M. Danos, *Nuclear Physics* **5**, 23 (1958).
- [69] K. Okamoto, Intrinsic quadrupole moment and the resonance width of photonuclear reactions, *Phys. Rev.* **110**, 143 (1958).
- [70] M. Guttormsen, Y. Alhassid, W. Ryssens, K. Ay, M. Ozgur, E. Algin, A. Larsen, F. Bello Garrote, L. Crespo Campo, T. Dahl-Jacobsen, A. Görge, T. Hagen, V. Ingeberg, B. Kheswa, M. Klintefjord, J. Midtbø, V. Modamio, T. Renstrøm, E. Sahin, S. Siem, G. Tveten, and F. Zeiser, *Phys. Lett. B* **816**, 136206 (2021).